8
Modal Testing

8.1 INTRODUCTION

This chapter introduces the basic topics associated with dynamic measurement and testing of structures. In the previous chapters, the differential equations, or models, of the system were assumed to be known, and the theory developed consists of calculating and characterizing the response of the system to known inputs. This is called the *forward problem*. In this chapter, however, the interest lies in measuring the response of a structure and in some way determining the equations of motion from test data. The problem of determining a system of equations from information about inputs and responses belongs to a class of problems called *inverse problems*. Although measurements of vibrating systems are made for a variety of reasons, this chapter focuses on the use of vibration measurement to identify, or verify, a mathematical model of a test structure. Other uses of vibration measurements include environmental testing, balancing of rotating machinery, prediction of failures, structural health monitoring, and machinery diagnostics for maintenance (Inman *et al.*, 2005).

The previous chapters have considered only structures modeled by lumped-mass elements. As mentioned in Section 2.5, however, many structures are not configured in clear, simple lumped-mass arrangements but rather have mass distributed throughout the structure. Such distributed-mass models form the topics of Chapters 9 through 13. However, measurements of distributed-mass structures often result in data that resemble the response of a lumped-mass structure. Hence, many test procedures, including those described here, assume that the structure being tested can be adequately described by a lumped-parameter model. The significance of such an assumption is discussed in Chapter 13 on finite-dimensional modeling of distributed-parameter systems.

There are several other assumptions commonly made but not stated (or understated) in vibration testing. The most obvious of these is that the system under test is linear and is driven by the test input only in its linear range. This assumption is essential and should not be neglected. Measurement of nonlinear systems is presented in Virgin (2000).

Vibration testing and measurement for modeling purposes forms a large industry. This field is referred to as *modal testing*, *modal analysis*, or *experimental modal analysis* (abbreviated EMA). Understanding modal testing requires knowledge of several areas. These include instrumentation, signal processing, parameter estimation, and vibration analysis. These topics are introduced in the following sections, but Ewins (2000) should be consulted for a complete description.

Vibration with Control D. J. Inman
© 2006 John Wiley & Sons, Ltd. ISBN: 0-470-01051-7

It is worth noting that modal testing activity is centered mainly around determining the modal parameters of a lumped-parameter model of the test structure. The process of determining a mathematical model of a system from measured inputs and outputs is called *system identification theory*. This theory has grown rapidly in the discipline of control theory rather than vibrations. System identification theory, in turn, is a subclass of inverse problems, as opposed to the direct problem discussed in earlier chapters. Much of the early work in modal analysis did not take advantage of the disciplines of system identification and parameter estimation, a situation rectified by efforts such as the book by Juang (1994). In the material that follows, a few of the basic approaches are presented.

As mentioned, the first seven chapters consider only the *forward problem*, i.e., given the matrices M, D, and K along with the appropriate initial conditions and forcing functions, determine the solution of Equation (2.13) describing the dynamics of the structure. The *inverse problem*, on the other hand, is to determine the matrices M, D, and K from knowledge of the measurements of the responses (position, velocity, or acceleration). The modal testing problem, a subclass of inverse problems, is to recover the mode shapes, natural frequencies, and damping ratios from response measurements. In general, modal testing methods cannot fully determine the matrices of physical parameters M, D, and K. While forward problems have a unique solution for linear systems, inverse problems do not. Model updating, introduced in Section 8.8, is an attempt to justify the analytically derived values of M, D, and K with measured modal data.

The fundamental idea behind modal testing is that of resonance first introduced in Section 1.4. If a structure is excited at resonance, its response exhibits two distinct phenomena, as indicated by Equations (1.19) and (1.20). As the driving frequency approaches the natural frequency of the structure, the magnitude at resonance rapidly approaches a sharp maximum value, provided the damping ratio is less than about 0.5. The second, often neglected, phenomenon of resonance is that the phase of the response shifts by 180° as the frequency sweeps through resonance, with the value of the phase at resonance being 90°.

The first few sections of this chapter deal with the hardware considerations and digital signal analysis necessary for making a vibration measurement for any purpose. The data acquisition and signal processing hardware has changed considerably over the past decade and continues to change rapidly as a result of advances in solid-state and computer technology. The remaining sections discuss the modal analysis version of model identification and parameter estimation. The last section introduces model updating.

8.2 MEASUREMENT HARDWARE

A vibration measurement generally requires several hardware components. The basic hardware elements required consist of a source of excitation for providing a known or controlled input to the structure, a *transducer* to convert the mechanical motion of the structure into an electrical signal, a signal conditioning amplifier to match the characteristics of the transducer to the input electronics of the digital data acquisition system, and an analysis system (or analyzer), in which signal processing and modal analysis programs reside. The arrangement is illustrated in Figure 8.1; it includes a power amplifier and a signal generator for the exciter, as well as a transducer to measure, and possibly control, the driving force or other input. Each of these devices and their functions are discussed briefly in this section.

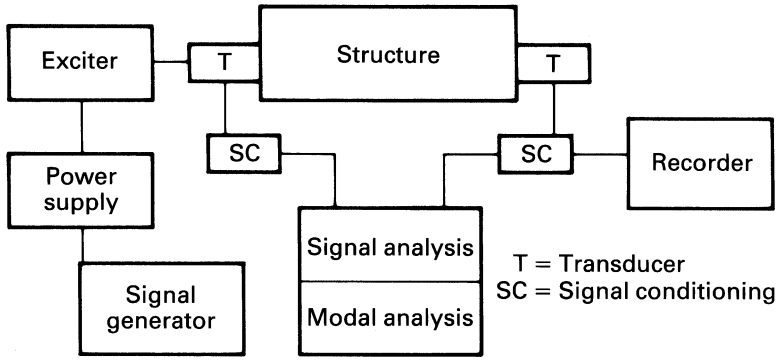

Figure 8.1 Components of a vibration measurement system for modal analysis.

First consider the excitation system, denoted 'exciter' in Figure 8.1. This system provides an input motion or, more commonly, a driving force $f_i(t)$, as in Equation (2.13). The physical device may take several forms, depending on the desired input and the physical properties of the test structure. The two most commonly used exciters in modal testing are the shaker (electromagnetic or electrohydraulic) and the impulse hammer. The preferred device is often the electromagnetic exciter, which has the ability, when properly sized, to provide inputs large enough to result in easily measured responses. Also, the output is easily controlled electronically, sometimes using force feedback. The excitation signal, which can be tailored to match the requirements of the structure being tested, can be a swept sine, random, or other appropriate signal. The *electromagnetic shaker* is basically a linear electric motor consisting of coils of wire surrounding a shaft in a magnetic field. An alternating current applied to the coil causes a force to be applied to the shaft, which, in turn, transfers force to the structure. The input electrical signal to the shaker is usually a voltage that causes a proportional force to be applied to the test structure.

Since shakers are attached to the test structure and since they have significant mass, care should be taken by the experimenter in choosing the size of shaker and method of attachment to minimize the effect of the shaker on the structure. The shaker and its attachment can add mass to the structure under test (called *mass loading*) as well as otherwise constraining the structure.

Mass loading and other constraints can be minimized by attaching the shaker to the structure through a *stinger*. A stinger consists of a short thin rod (usually made of steel or nylon) running from the driving point of the shaker to a force transducer mounted directly on the structure. The stinger serves to isolate the shaker from the structure, reduces the added mass, and causes the force to be transmitted axially along the stinger, controlling the direction of the applied force.

Excitation can also be applied by an *impulse* by using an *impact hammer*. An impact hammer consists of a hammer with a force transducer built into its head. The hammer is then used to hit (impact) the test structure and thus excite a broad range of frequencies. The peak impact force is nearly proportional to the hammer head mass and the impact velocity. The upper frequency limit excited by the hammer is decreased by increasing the hammer head mass, and increased with increasing stiffness of the tip of the hammer.

As a simple example of how the choice of excitation device is critical, consider Figure 8.2. This plot illustrates the frequency spectrum of a typical force resulting from a hammer

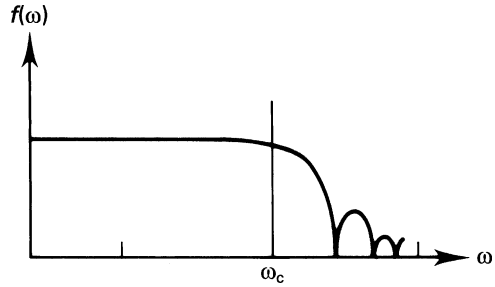

Figure 8.2 Frequency spectrum of a typical hammer impact.

impact or hit. It shows that the impact force is approximately constant up to a certain value of frequency, denoted by ω_c. This hammer hit is less effective in exciting the modes of the structure with frequencies larger than ω_c than it is in exciting the modes with frequencies less than ω_c. For a given hammer mass, ω_c can be lowered by using a softer tip.

The built-in force transducer in impact hammers should be dynamically calibrated for each tip used, as this will affect the sensitivity. Although the impact hammer is simple and does not add mass loading to the structure, it is often incapable of transforming sufficient energy to the structure to obtain adequate response signals in the frequency range of interest. Also, peak impact loads are potentially damaging, and the direction of the applied load is difficult to control. Nonetheless, impact hammers remain a popular and useful excitation device, as they generally are much faster to use than shakers.

Next, consider the transducers required to measure the response of the structure as well as the impact force. The most popular and widely used transducers are made from piezoelectric materials. Piezoelectric materials generate electrical charge when strained. By various designs, transducers incorporating these materials can be built to produce signals proportional to either force or local acceleration. *Accelerometers*, as they are called, actually consist of two masses, one of which is attached to the structure, separated by a piezoelectric material, which acts like a very stiff spring. This causes the transducer to have a resonant frequency. The maximum measurable frequency is usually a fraction of the resonance frequency of the accelerometer. In fact, the upper frequency limit is usually determined by the so-called mounted resonance, since the connection of the transducer to the structure is always somewhat compliant.

Piezoelectric materials also produce a strain when excited with a voltage. Hence, piezoelectric materials are emerging as a reasonable means of vibration excitation for special-purpose situations, as described, for instance, by Cole, Saunders, and Robertshaw (1995) and Inman *et al.* (2005).

The output impedance of most transducers is not well suited for direct input into signal analysis equipment. Hence, *signal conditioners*, which may be charge amplifiers or voltage amplifiers, match and often amplify signals prior to analyzing the signal. It is very important that each set of transducers along with signal conditioning is properly calibrated in terms of both magnitude and phase over the frequency range of interest. While accelerometers are convenient for many applications, they provide weak signals if one is interested in lower-frequency vibrations incurred in terms of velocity of displacement. Even substantial low-frequency vibration displacements may result in only small accelerations, recalling that, for a harmonic displacement of amplitude X, the acceleration amplitude is $-\omega^2 X$. Strain gauges

and potentiometers as well as various optical (fiber optics, laser vibrometers), capacitive, and inductive transducers are often more suitable than accelerometers for low-frequency motion measurement.

Once the response signal has been properly conditioned, it is routed to an analyzer for signal processing. The standard is called a digital or discrete Fourier analyzer (often abbreviated DFA), also called the fast Fourier transform (often abbreviated FFT) analyzer; and is introduced briefly here. Basically, the DFA accepts analog voltage signals which represent the acceleration (force, velocity, displacement, or strain) from a signal conditioning amplifier. This signal is filtered and digitized for computation. Discrete frequency spectra of individual signals and cross-spectra between the input and various outputs are computed. The analyzed signals can then be manipulated in a variety of ways to produce such information as natural frequencies, damping ratios, and mode shapes in numerical or graphic displays.

While almost all the commercially available analyzers are marketed as turnkey devices, it is important to understand a few details of the signal processing performed by these analysis units in order to carry out valid experiments. This forms the topic of the next two sections.

8.3 DIGITAL SIGNAL PROCESSING

Much of the analysis done in modal testing is performed in the frequency domain, as discussed in Section 5.7. The analyzer's task is to convert analog time domain signals into digital frequency domain information compatible with digital computing and then to perform the required computations with these signals. The method used to change an analog signal, $x(t)$, into frequency domain information is the Fourier transform (similar to the Laplace transform used in Chapter 5), or a *Fourier series*. The Fourier series is used here to introduce the digital Fourier transform (DFT). See Newland (1985, p. 38) for the exact relationship between a Fourier transform and a Fourier series.

Any periodic in time signal, $x(t)$, of period T can be represented by a Fourier series of the form

$$x(t) = \frac{a_0}{2} + \sum_{i=1}^{\infty} \left[a_i \cos \frac{2\pi i t}{T} + b_i \sin \frac{2\pi i t}{T} \right] \tag{8.1}$$

where the constants a_i and b_i, called the *Fourier coefficients*, or *spectral coefficients*, are defined by

$$\begin{aligned} a_i &= \frac{2}{T} \int_0^T x(t) \cos \frac{2\pi i t}{T} dt \\ b_i &= \frac{2}{T} \int_0^T x(t) \sin \frac{2\pi i t}{T} dt \end{aligned} \tag{8.2}$$

The expression in Equation (8.1) is referred to as the Fourier series for the periodic function $x(t)$. The spectral coefficients represent frequency domain information about the time signal $x(t)$.

The coefficients a_i and b_i also represent the connection to vibration experiments. The analog output signals of accelerometers and force transducers, represented by $x(t)$, are inputs to the analyzer. The analyzer in turn calculates the spectral coefficients of these signals,

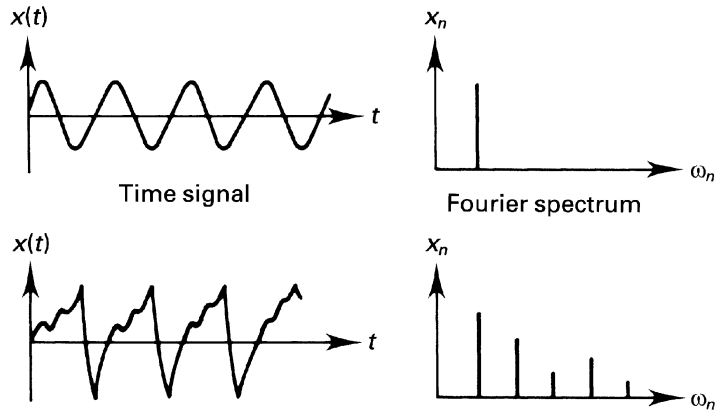

Figure 8.3 Some signals and their Fourier spectrum.

thus setting the stage for a frequency domain analysis of the signals. Some signals and their Fourier spectrum are illustrated in Figure 8.3. The analyzer first converts the analog signals into digital records. It samples the signals $x(t)$ at many different equally spaced values and produces a digital record of the signal in the form of a set of numbers $\{x(t_k)\}$. Here, $k = 1, 2, \ldots, N$, the digit N denotes the number of samples, and t_k indicates a discrete value of the time.

This process is performed by an analog-to-digital converter (often denoted by A/D). This conversion from an analog to digital signal can be thought of in two ways. First, one can imagine a grate that samples the signal every t_k seconds and passes through the signal $x(t_k)$. One can also consider the analog-to-digital converters as multiplying the signal $x(t)$ by a square-wave function, which is zero over alternate values of t_k and has the value of 1 at each t_k for a short time. Some signals and their digital representation are illustrated in Figure 8.4.

In calculating digital Fourier transforms, one must be careful in choosing the sampling time, i.e., the time elapsed between successive t_k. A common error introduced in digital signal analysis caused by improper sampling time is called *aliasing*. Aliasing results from analog-to-digital conversion and refers to the misrepresentation of the analog signal by the digital record. Basically, if the sampling rate is too slow to catch the details of the analog

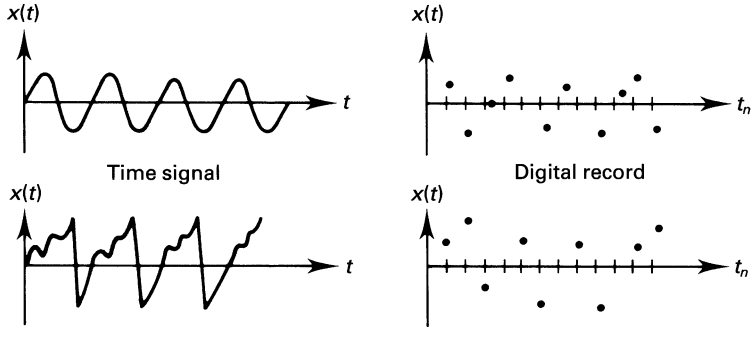

Figure 8.4 Sample time histories and their corresponding digital record.

signal, the digital representation will cause high frequencies to appear as low frequencies. The following example illustrates two analog signals of different frequency that produce the same digital record.

Example 8.3.1

Consider the signals $x_1(t) = \sin[(\pi/4)t]$ and $x_2(t) = -\sin[(7\pi/4)t]$, and suppose these signals are both sampled at 1 intervals. The digital record of each signal is given in the following table.

t_k	0	1	2	3	4	5	6	7	ω_i
x_1	0	0.707	1	0.707	0	−0.707	−1	−0.707	$\frac{1}{8}$
x_2	0	0.707	1	0.707	0	−0.707	−1	−0.707	$\frac{7}{8}$

As is easily seen from the table, the digital sample records of x_1 and x_2 are the same, i.e., $x_1(t_k) = x_2(t_k)$ for each value of k. Hence, no matter what analysis is performed on the digital record, x_1 and x_2 will appear the same. Here, the sampling frequency, $\Delta\omega$, is 1. Note that $\omega_1 - \Delta\omega = 1/8–1 = -7/8$, which is the frequency of $x_2(t)$.

To avoid aliasing, the sampling interval, denoted by Δt, must be chosen small enough to provide at least two samples per cycle of the highest frequency to be calculated. That is, in order to recover a signal from its digital samples, the signal must be sampled at a rate at least twice the highest frequency in the signal. In fact, experience (see Otnes and Enochson, 1972) indicates that 2.5 samples per cycle is a better choice. This is called the *sampling theorem*, or *Shannon's sampling theorem*.

Aliasing can be avoided in signals containing many frequencies by subjecting the analog signal $x(t)$ to an *antialiasing* filter. An antialiasing filter is a low-pass (i.e., only allowing low frequencies through) sharp cut-off filter. The filter effectively cuts off frequencies higher than about half the maximum frequency of interest, denoted by $\omega_{\max}$, and also called the *Nyquist frequency*. Most digital analyzers provide built-in antialiasing filters.

Once the digital record of the signal is available, the discrete version of the Fourier transform is performed. This is accomplished by a digital Fourier transform or series defined by

$$x_k = x(t_k) = \frac{a_0}{2} + \sum_{i=1}^{N/2}\left[a_i \cos\frac{2\pi i t_k}{T} + b_i \sin\frac{2\pi i t_k}{T}\right], \qquad k = 1, 2, \ldots, N \tag{8.3}$$

where the *digital spectral coefficients* are given by

$$\begin{aligned} a_0 &= \frac{1}{N}\sum_{k=1}^{N} x_k \\ a_i &= \frac{1}{N}\sum_{k=1}^{N} x_k \cos\frac{2\pi i k}{N} \\ b_i &= \frac{1}{N}\sum_{k=1}^{N} x_k \sin\frac{2\pi i k}{N} \end{aligned} \tag{8.4}$$

The task of the analyzer is to solve Equations (8.3) given the digital record $x(t_k)$, also denoted by x_k, for the measured signals. The transform size or number of samples, N, is usually fixed for a given analyzer and is a power of 2.

Writing out Equations (8.3) for each of the N samples yields N linear equations in the N spectral coefficients $(a_1, \ldots, a_{N/2}, b_1, \ldots, b_{N/2})$. These equations can also be written in the form of matrix equations. Equations (8.3) in matrix form become

$$\mathbf{x} = C\mathbf{a} \tag{8.5}$$

where $\mathbf{x}$ is the vector of samples with elements x_k and $\mathbf{a}$ is the vector of spectral coefficients. The solution of Equations (8.5) for the spectral coefficients is then given simply by

$$\mathbf{a} = C^{-1}\mathbf{x} \tag{8.6}$$

The task of the analyzer is to compute C^{-1} and hence the coefficients $\mathbf{a}$. The most widely used method of computing the inverse of this matrix C is called the fast Fourier transform (FFT) developed by Cooley and Tukey (1965).

In order to make digital analysis feasible, the periodic signal must be sampled over a finite time (N must obviously be finite). This can give rise to another problem referred to as *leakage*. To make the signal finite, one could simply cut the signal at any integral multiple of its period. Unfortunately, there is no convenient way to do this for complicated signals containing many different frequencies. Hence, if no further steps are taken, the signal may be cut off midperiod. This causes erroneous frequencies to appear in the digital representation because the digital Fourier transform of the finite-length signal assumes that the signal is periodic within the sample record length. Thus, the actual frequency will 'leak' into a number of fictitious frequencies. This is illustrated in Figure 8.5.

Leakage can be corrected to some degree by the use of a *window function*. Windowing, as it is called, involves multiplying the original analog signal by a weighting function, or window function, $w(t)$, which forces the signal to be zero outside the sampling period.

A common window function, called the *Hanning window*, is illustrated in Figure 8.6, along with the effect it has on a periodic signal. A properly windowed signal will yield a spectral plot with much less leakage. This is also illustrated in the figures.

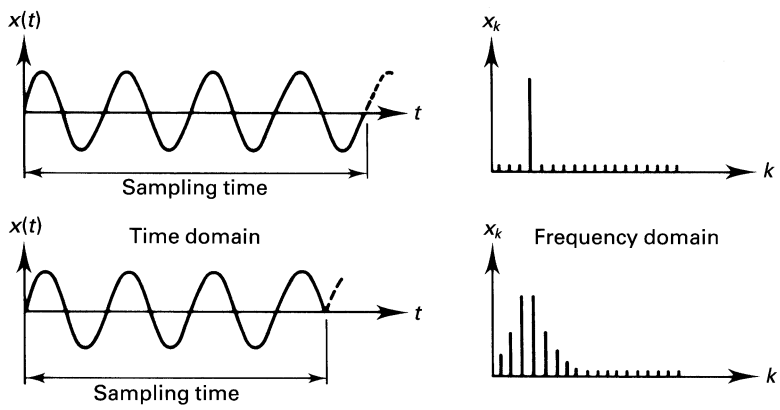

Figure 8.5 Illustration of leakage.

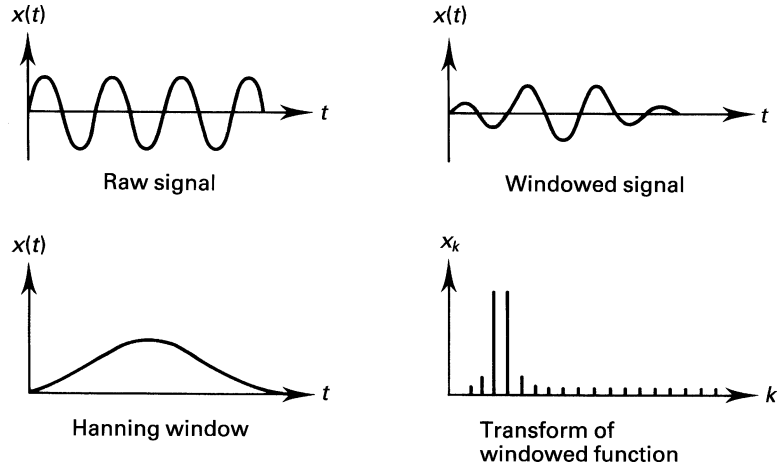

Figure 8.6 Hanning window and its effect on transform signals.

8.4 RANDOM SIGNAL ANALYSIS

This section introduces the topic of transfer function identification from signals, which is the most commonly used approach to system identification concerned with trying to determine the modal parameters of a linear time-invariant system. In most test situations, it becomes desirable to average measurements to increase confidence in the measured parameter. This, along with the fact that a random excitation is often used in testing, requires some background in random processes.

First, some concepts and terminology required to describe random signals need to be established. Consider a random signal $x(t)$ such as pictured in Figure 8.7. The first distinction to be made about a random time history is whether or not the signal is stationary. A random signal is *stationary* if its statistical properties (such as its root mean square value, defined later) are time-independent (i.e., do not change with time). For random signals, it is not possible to focus on the details of the signal, as it is with a pure deterministic signal. Hence, random signals are classified and manipulated in terms of their statistical properties.

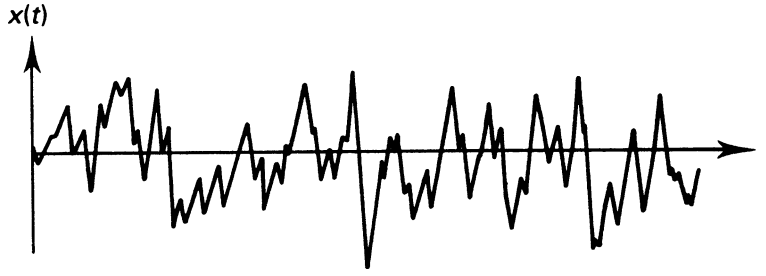

Figure 8.7 Sample random signal.

The *average* of the random signal $x(t)$ is defined and denoted by

$$\overline{x}(t) = \lim_{T\to\infty} \frac{1}{T}\int_0^T x(t)\,dt \tag{8.7}$$

For a digital signal, the definition of average becomes

$$\overline{x} = \lim_{N\to\infty} \frac{1}{N}\sum_{k=1}^{N} x(t_k) \tag{8.8}$$

Often, it is convenient to consider signals with zero average, or *mean*, i.e., $\overline{x}(t) = 0$. This is not too restrictive an assumption, since, if $\overline{x}(t) \neq 0$, a new variable $x' = x(t) - \overline{x}(t)$ can be defined. The new variable $x'(t)$ now has zero mean. In what follows, the signals are assumed to have zero mean.

The *mean square value* of the random variable $x(t)$ is denoted by $\overline{x}^2(t)$ and is defined by

$$\overline{x}^2 = \lim_{T\to\infty} \frac{1}{T}\int_0^T x^2(t)\,dt \tag{8.9}$$

or, in digital form,

$$\overline{x}^2 = \lim_{N\to\infty} \frac{1}{N}\sum_{k=1}^{N} x^2(t_k) \tag{8.10}$$

The mean square value, or *variance* as it is often called, provides a measure of the magnitude of the fluctuations in the signal. A related quantity, called the *root mean square* value, or simply the RMS value, of $x(t)$ is just the square root of the variance, i.e.,

$$x_{\mathrm{RMS}} = \sqrt{\overline{x}^2} \tag{8.11}$$

Another question of interest for a random variable is that of calculating the probability that the variable $x(t)$ will lie in a given interval. However, neither the root mean square value of $x(t)$ nor its probability yields information about how 'fast' the values of $x(t)$ change and hence how long it takes to measure enough $x(t_k)$ to compute statistically meaningful root mean square values and probabilities. A measure of the speed with which the random variable $x(t)$ is changing is provided in the time domain by the *autocorrelation* function. For analog signals, the autocorrelation function, denoted by $R(t)$, defined by

$$R(t) = x^2 = \lim_{T\to\infty} \frac{1}{T}\int_0^T x(\tau)x(\tau+t)\,d\tau \tag{8.12}$$

is used as a measure of how fast the signal $x(t)$ is changing. Note that $R(0)$ is the mean square value of $x(t)$. The autocorrelation function is also useful for detecting the presence of periodic signals contained in, or buried in, random signals. If $x(t)$ is periodic or has a periodic component, then $R(t)$ will be periodic instead of approaching zero as $T \to \infty$, as required for a purely random $x(t)$.

The digital form of the autocorrelation function is

$$R(r, \Delta t) = \frac{1}{N-r}\sum_{k=0}^{N-r} x_k x_{k+r} \tag{8.13}$$

Here, N is the number of samples, Δt is the sampling interval, and r is an adjustable parameter, called a *lag value*, that controls the number of points used to calculate the autocorrelation function.

In the frequency domain, the *power spectral density* (often denoted PSD) is used to measure the speed with which the random variable $x(t)$ changes. The power spectral density, denoted by $S(\omega)$, is defined to be the Fourier transform of $R(t)$, i.e.,

$$S(\omega) = \frac{1}{2\pi} \int_{-\infty}^{\infty} R(\tau)\, e^{-j\omega\tau}\, d\tau \tag{8.14}$$

The digital version of the power spectral density is given by

$$S(\Delta\omega) = \frac{|x(\omega)|^2}{N\,\Delta t} \tag{8.15}$$

where $|x(\omega)|^2$ is the magnitude of the Fourier transform of the sampled data corresponding to $x(t)$.

This definition of the autocorrelation function can also be applied to two different signals to provide a measure of the transfer function between the two signals. The *cross-correlation* function, denoted by $R_{xf}(t)$, for the two signals $x(t)$ and $f(t)$ is defined to be

$$R_{xf}(t) = \lim_{T\to\infty} \frac{1}{T} \int_{0}^{T} x(\tau) f(\tau + t)\, d\tau \tag{8.16}$$

Likewise, the *cross-spectral density* is defined as the Fourier transform of the cross-correlation, i.e.,

$$S_{xf}(\omega) = \frac{1}{2\pi} \int_{-\infty}^{\infty} R_{xf}(\tau)\, e^{-j\omega\tau}\, d\tau \tag{8.17}$$

If the function $f(\tau + t)$ is replaced with $x(\tau + t)$ in Equation (8.16), the power spectral density [Equation (8.14)], also denoted by S_{xx}, results. These correlation and density functions allow calculation of the transfer functions of test structures. The frequency response function (recall Section 1.5), $G(j\omega)$, can be shown (see, for instance, Ewins, 2000) to be related to the spectral density functions by the two equations

$$S_{fx}(\omega) = G(j\omega) S_{ff}(\omega) \tag{8.18}$$

and

$$S_{xx}(\omega) = G(j\omega) S_{xf}(\omega) \tag{8.19}$$

These hold if the structure is excited by a random input f resulting in the response x. Here, S_{ff} denotes the power spectral density for the function $f(t)$, which is taken to be the excitation force in a vibration test.

The spectrum analyzer calculates (or estimates) the various spectral density functions. Then, using Equation (8.18) or (8.19), the analyzer can calculate the desired frequency response function $G(j\omega)$. Note that Equations (8.18) and (8.19) use different power spectral densities to calculate the same quantity. This can be used to check the value of $G(j\omega)$.

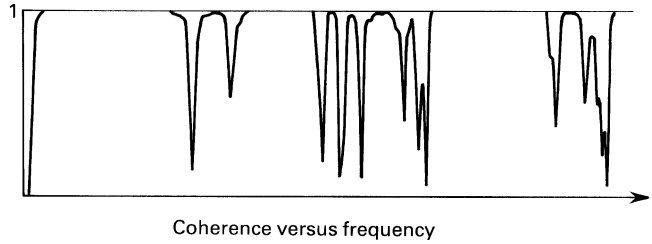

Figure 8.8 Plot of the coherence of a sample signal versus frequency.

The *coherence function*, denoted by γ^2, is defined to be the ratio of the two values of $G(j\omega)$ calculated from Equations (8.18) and (8.19). Let $G'(j\omega) = S_{fx}(\omega)/S_{ff}(\omega)$ denote the value of G obtained from Equation (8.18) from measurements of $S_{fx}(\omega)$ and $S_{ff}(\omega)$. Likewise, let $G''(j\omega) = S_{xx}(\omega)/S_{fx}(\omega)$ denote the frequency response as determined by measurements made for Equation (8.19). Then the coherence function becomes

$$\gamma^2 = \frac{G'(j\omega)}{G''(j\omega)} \tag{8.20}$$

which is always less than or equal to 1. In fact, if the measurements are consistent, $G(j\omega)$ should be the same value, independent of how it is calculated, and the coherence should be 1 ($\gamma^2 = 1$). In practice, coherence versus frequency is plotted (see Figure 8.8) and is taken as an indication of how accurate the measurement process is over a given range of frequencies. Generally, the values of $\gamma^2 = 1$ should occur at values of ω near the resonant frequencies of the structure.

8.5 MODAL DATA EXTRACTION (FREQUENCY DOMAIN)

Once the frequency response of a test structure is calculated from Equation (8.18) or (8.19), the analyzer is used to construct various vibrational information from the processed measurements. This is what is referred to as *experimental modal analysis*. In what follows, it is assumed that the frequency response function $G(j\omega)$ has been measured via Equation (8.18) or (8.19) or their equivalents.

The task of interest is to measure the natural frequencies, damping ratios, and modal amplitudes associated with each resonant peak of the frequency response function. There are several ways to examine the measured frequency response function to extract the desired modal data. To examine all of them is beyond the scope of this text. To illustrate the basic method, consider the somewhat idealized frequency response function record of Figure 8.9, resulting from measurements taken between two points on a simple structure.

One of the gray areas in modal testing is deciding on the number of degrees of freedom to assign to a test structure. In many cases, simply counting the number of clearly defined peaks or resonances, three in Figure 8.9, determines the order, and the procedure continues with a three-mode model. However, as is illustrated later on, this procedure may not be accurate if the structure has closely spaced natural frequencies or high damping values.

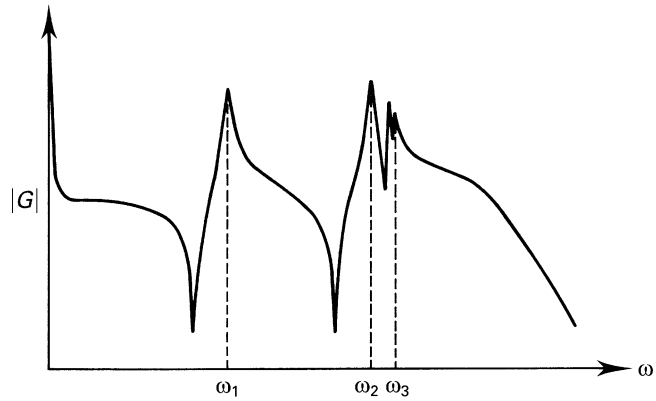

Figure 8.9 Idealized frequency response function.

The easiest method to use on these data is the so-called single-degree-of-freedom curve fit (often called the SDOF method), an approach alluded to in Section 2.5. In this approach the frequency response function is sectioned off into frequency ranges bracketing each successive peak. Each peak is then analyzed by assuming it is the frequency response of a single-degree-of-freedom system. This assumes that, in the vicinity of the resonance, the frequency response function is dominated by that single mode.

In other words, in the frequency range around the first resonant peak, it is assumed that the curve is due to the response of a damped single-degree-of-freedom system to a harmonic input at and near the first natural frequency. Recall from Section 1.4 that the point of resonance corresponds to that value of frequency for which the magnification curve has its maximum or peak value and the phase changes 180°.

The method is basically the peak picking method referred to in Section 1.6 and illustrated in Figure 1.8. The approach is to assume that the peak occurs at the frequency corresponding to the damped natural frequency of that particular mode, denoted by ω_{di} (for the ith mode). The two frequencies on each side of this peak correspond to the points on the curve that are 0.707 of $|G(j\omega_{di})|$ (also called the half-power points). Denoting these two frequencies as ω_{1i} and ω_{2i}, the formula for calculating the damping ratio for the ith peak is (see Blevins, 1994, p. 318)

$$\zeta_i = \frac{\omega_{2i} - \omega_{1i}}{2\omega_{di}} \tag{8.21}$$

Next, even though these formulae result from examining a single-degree-of-freedom model, it is recognized that the system is a distributed mass system that is being modeled as a multiple-degree-of-freedom system with three modes. The frequency response function for a multiple-degree-of-freedom system is discussed in Section 5.7 and leads to the concept of a receptance matrix, $\alpha(\omega)$, which relates the input vector (driving force) to the response (position in this case) via Equation (5.67). For a three-degree-of-freedom system, with the assumption of proportional damping and that the frequency response near resonance ω_{d1} is not influenced by contributions from ω_{d2} and ω_{d3}, the magnitude of the measured frequency response at ω_{d1}, denoted by $G(j\omega_{d1})$, allows the calculation of one of the elements of the receptance matrix.

If the structure is underdamped, the ikth element of the receptance matrix is given by

$$\alpha_{ik} = \sum_{r=1}^{n} \frac{[\mathbf{s}_r \mathbf{s}_r^T]_{ik}}{\omega_r^2 + 2j\zeta_r \omega_r \omega - \omega^2} \tag{8.22}$$

where $\mathbf{s}_r$ is the rth eigenvector of the system. The magnitude of $\alpha_{ij}(\omega_r)$ is the measured amplitude of the peak at ω_r. In this case, Equation (8.22) becomes

$$\alpha_{ik}(\omega_r) = \frac{[\mathbf{s}_r \mathbf{s}_r^T]_{ik}}{\omega_r^2 + 2\zeta_r \omega_r^2 j - \omega_r^2} \tag{8.23}$$

Hence

$$\left|[\mathbf{s}_r \mathbf{s}_r^T]_{ik}\right| = |G_{ik}(j\omega_r)| \left|2\zeta_r \omega_r^2 j\right| = 2\zeta_r \omega_r^2 \, |G_{ik}(j\omega_r)| \tag{8.24}$$

Here, the measured value of the maximum of the frequency response function at $\omega_r = \omega$ with input at point i and response measured at point k is denoted by $G_{ik}(\omega)$ and is approximated by $|\alpha_{ik}(\omega)|$. With the assumption, stated earlier, that the response is due to only one frequency near resonance, Equation (8.24) yields one value for the *modal constant*, which is defined as the magnitude of the ikth element of the matrix $\mathbf{s}_1 \mathbf{s}_1^T$. The phase plot yields the relative sign of the ikth element of $\mathbf{s}_1 \mathbf{s}_1^T$. Equation (8.24) is the mathematical equivalent of assuming that the first peak in the curve of Figure 8.9 results from only a single-degree-of-freedom system.

The subscripts ik denote the output coordinate and the relative position of the input force. In order words, the quantity $|\alpha_{ik}(\omega_r)|$ represents the magnitude of the transfer function between an input at point i and a measured output at point k.

Here, an estimate of the eigenvectors, or mode shapes, can be calculated by making a series of measurements at different points, applying the modal constant formula, [Equation (8.24)], and examining the relative phase shift at ω_{di}. To see this, suppose that the transfer function of Figure 8.9 is between the input f_1 (at point 1) and the measured response x_3 (at point 3 on the structure as labeled in Figure 8.10). Then, from Equation (8.24) with $i = 1, k = 3$, and $r = 1, 2, 3$, the three values of the matrix elements $\left[\mathbf{s}_1 \mathbf{s}_1^T\right]_{13}$, $\left[\mathbf{s}_2 \mathbf{s}_2^T\right]_{13}$, and $\left[\mathbf{s}_3 \mathbf{s}_3^T\right]_{13}$ can be measured. Furthermore, if the preceding experiment is completed two more times with the response measurement (or the force) being moved to the two remaining positions ($k = 2, 1$) shown in Figure 8.10, the following matrix elements can also be measured: $\left[\mathbf{s}_1 \mathbf{s}_1^T\right]_{12}$, $\left[\mathbf{s}_2 \mathbf{s}_2^T\right]_{12}$, and $\left[\mathbf{s}_3 \mathbf{s}_3^T\right]_{12}$ as well as $\left[\mathbf{s}_1 \mathbf{s}_1^T\right]_{11}$, $\left[\mathbf{s}_2 \mathbf{s}_2^T\right]_{11}$, and $\left[\mathbf{s}_3 \mathbf{s}_3^T\right]_{11}$. Gathering up these nine elements of the three different outer product matrices $\mathbf{s}_1 \mathbf{s}_1^T$, $\mathbf{s}_2 \mathbf{s}_2^T$, and $\mathbf{s}_3 \mathbf{s}_3^T$ allows the three vectors $\mathbf{s}_1$, $\mathbf{s}_2$, and $\mathbf{s}_3$ to be calculated (problem 8.5). Note that, because of its special structure, knowing one row or one column of the matrix $\mathbf{s}_i \mathbf{s}_i^T$ is enough to determine the entire matrix and hence the value of $\mathbf{s}_i$ to within a multiplicative constant.

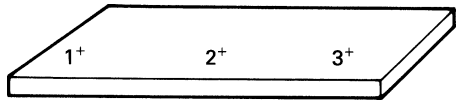

Figure 8.10 Measurement positions marked on a simple plate for performing a modal test.

Hence, through measurements taken from the plot in Figure 8.9, along with the above computations and two more measurements at the remaining two measurement points, the receptance matrix, given by Equation (5.68), is completely determined, as are the eigenvalues and eigenvectors of the system. However, in general this does *not* provide enough information to determine the values of the matrices M, D, and K, because the eigenvectors may not be scaled (normalized) properly. Also, the mathematical model constructed in this way is dependent upon the choice of measurement points and as such should not be considered to be unique.

Given the modal data, however, the receptance matrix can be used to predict the response of the system as the result of any input, to compare the modal data with theoretical models, or, along with other information, to construct physical models of the structure. The question of uniqueness remains, and the physical models developed should always be referenced to the measurement and disturbance position used in performing the test.

The single-degree-of-freedom method is really not based on a principle of parameter identification but rather is an unsophisticated first attempt to 'read' the experimental data and to fit the data into a specific underdamped vibration model. An attempt to make the single-degree-of-freedom approach more sophisticated is to plot the real part of the frequency response function versus the imaginary part near the resonant frequency. This yields the Nyquist plot of Figure 1.14. In this domain, the theory predicts a circle; hence, the experimental data around a resonant peak can be 'fit' using a least-squares circle fit to produce the 'best' circle for the given data. Then the frequency and damping values can be taken from the Nyquist plot. This method is referred to as the *circle fit method* and brings the problem a little closer to using the science of parameter estimation (see Ewins, 2000, or Zaveri, 1984, for a more complete account).

The single-degree-of-freedom method is in obvious error for systems with closely spaced modes and/or highly coupled modes. Hence, several other methods have been developed to take into consideration the effects of coupling. These methods are usually referred to as multiple-degree-of-freedom curve fits and consist largely of adding correction terms to Equation (8.23) to take into consideration mode coupling effects. Because of space limitations, these methods are not discussed here. The reader is referred to the note section at the end of the chapter for references to more advanced methods.

8.6 MODAL DATA EXTRACTION (TIME DOMAIN)

An alternative approach to extracting the modal data of a structure from the vibrational response of the structure is based in the time domain. Time domain methods have been more successful in identifying closely spaced or repeated natural frequencies. They also offer a more systematic way of determining the appropriate order (number of degrees of freedom) of a test structure and generally identify a larger number of natural frequencies than frequency domain methods do. Time domain methods are also referred to as damped complex exponential response methods (Allemang, 1984).

The first time domain method to make an impact on the vibration testing community was developed by Ibrahim (1973) and has since become known as the Ibrahim time domain (ITD) method. The original method is based on the state equations of a dynamic system [i.e., equation (2.20)]. A simplified version of the method is presented here.

The solution for the dynamic system in physical coordinates in the form of Equation (2.13) is given in Equation (3.68) and repeated here as

$$\mathbf{q}(t) = \sum_{r=1}^{2n} c_r \mathbf{r}_r e^{\lambda_r t} \tag{8.25}$$

where λ_r are the complex latent roots, or eigenvalues, of the system and the $\mathbf{u}_r$ are the system eigenvectors. Here, it is convenient to absorb the constant c_r into the vector $\mathbf{u}_r$ and write Equation (8.25) as

$$\mathbf{q}(t) = \sum_{r=1}^{2n} \mathbf{p}_r e^{\lambda_r t} \tag{8.26}$$

where the vector $\mathbf{p}_r$ has an arbitrary norm. If the response is measured at discrete times, t_i, then Equation (8.26) becomes simply

$$\mathbf{q}(t_i) = \sum_{r=1}^{2n} \mathbf{p}_r e^{\lambda_r t_i} \tag{8.27}$$

For simplicity of explanation, assume that the structure is measured in n places (this assumption can be relaxed) at $2n$ times, where n is the number of degrees of freedom exhibited by the test structure. Writing Equation (8.27) $2n$ times results in the matrix equation

$$X = PE(t_i) \tag{8.28}$$

where $\mathbf{X}$ is an $n \times 2n$ matrix with columns consisting of the $2n$ vectors $\mathbf{q}(t_1), \mathbf{q}(t_2), \ldots, \mathbf{q}(t_{2n})$, P is the $n \times 2n$ matrix with columns consisting of the $2n$ vectors $\mathbf{p}_r$, and $E(t_i)$ is the $2n \times 2n$ matrix given by

$$E(t_i) = \begin{bmatrix} e^{\lambda_1 t_1} & e^{\lambda_1 t_2} & \cdots & e^{\lambda_1 t_{2n}} \\ e^{\lambda_2 t_1} & e^{\lambda_2 t_2} & & e^{\lambda_2 t_{2n}} \\ \vdots & \vdots & & \vdots \\ e^{\lambda_{2n} t_1} & e^{\lambda_{2n} t_2} & \cdots & e^{\lambda_{2n} t_{2n}} \end{bmatrix} \tag{8.29}$$

Likewise, if these same responses are measured Δt seconds later, i.e., at time $t_i + \Delta t$, Equation (8.28) becomes

$$Y = PE(t_i + \Delta t) \tag{8.30}$$

where the columns of Y are defined by $\mathbf{y}(t_i) = \mathbf{q}(t_i + \Delta t)$, and $E(t_i + \Delta t)$ is the matrix with ijth element equal to $e^{\lambda_i (t_j + \Delta t)}$. Equation (8.30) can be factored into the form

$$Y = P' E(t_i) \tag{8.31}$$

where the matrix P' has as its ith column the vector $\mathbf{p}_i e^{\lambda_i \Delta t}$. This process can be repeated for another time increment Δt later to provide the equations

$$Z = P'' E(t_i) \tag{8.32}$$

where the columns of Z are the vectors $\mathbf{q}(t_i + 2\Delta t)$, and so on.

Collecting Equations (8.28) and (8.31) together yields

$$\Phi = \begin{bmatrix} X \\ Y \end{bmatrix} = \begin{bmatrix} P \\ P' \end{bmatrix} E(t_i) = \Psi E(t_i) \tag{8.33}$$

where the $2n \times 2n$ matrices Φ and Ψ have obvious definitions. Likewise, Equations (8.31) and (8.32) can be combined to form

$$\Phi' = \begin{bmatrix} Y \\ Z \end{bmatrix} = \begin{bmatrix} P' \\ P'' \end{bmatrix} E(t_i) = \Psi' E(t_i) \tag{8.34}$$

where $\Phi' = [Y^T \ Z^T]^T$ and $\Psi' = [P'^T \ P''^T]^T$. Note that the matrices Φ, Φ', Ψ, and Ψ' are all square $2n \times 2n$ matrices that are assumed to be nonsingular (Ibrahim and Mikulcik, 1976).

Equations (8.33) and (8.34) can be used to calculate a relationship between the vectors that make up the columns of the matrix Ψ and those of Ψ', namely

$$\Phi' \Phi^{-1} \Psi = \Psi' \tag{8.35}$$

so that

$$\Phi' \Phi^{-1} \Psi_i = \Psi_i', \qquad i = 1, 2, \ldots, 2n \tag{8.36}$$

where the subscript i denotes the ith column of the indexed matrix. However, the ith column of P' is $\mathbf{p}_i = e^{\lambda_i \Delta t}$, so that

$$\Psi_i' = e^{\lambda_i \Delta t} \Psi_i \tag{8.37}$$

Comparison of Equations (8.37) and (8.36) yields

$$\Phi' \Phi^{-1} \Psi_i = e^{\lambda_i \Delta t} \Psi_i \tag{8.38}$$

Note that this last expression states that the complex scalar $e^{\lambda_i \Delta t} = \beta + \gamma j$ is an eigenvalue of the matrix $\Phi' \Phi^{-1}$ with complex eigenvector Ψ_i. The $2n \times 1$ eigenvector Ψ_i has as its first n elements the eigenvector or mode shape of the structure. That is, $\Psi_i = [\mathbf{p}_i^T \quad \mathbf{p}_i^T e^{\lambda_i \Delta t}]^T$, where $\mathbf{p}_i$ are the system eigenvectors.

The eigenvalues of Equation (8.38) can be used to calculate the eigenvalues of the system and hence the damping ratios and natural frequencies. In particular, since $e^{\lambda_i \Delta t} = \beta + \gamma j$, it follows that

$$\mathrm{Re}\lambda_i = \frac{1}{\Delta t} \ln(\gamma^2 + \beta^2) \tag{8.39}$$

and

$$\mathrm{Im}\lambda_i = \frac{1}{\Delta t} \tan^{-1}\left(\frac{\gamma}{\beta}\right) \tag{8.40}$$

With proper consideration for sampling time and the interval for the arc tangent in Equation (8.40), Equation (8.38) yields the desired modal data.

To summarize, this method first constructs a matrix of measured time responses, forms the product $\Phi'\Phi^{-1}$, and then numerically calculates the eigenvalue–eigenvector problem for this matrix. The resulting calculation then yields the mode shapes, natural frequencies, and damping ratios of the structure. The natural frequencies and damping ratios follow from Equations (8.39) and (8.40) since (see Chapter 1)

$$\omega_i = [(\mathrm{Re}\lambda_i)^2 + (\mathrm{Im}\lambda_i)^2]^{1/2} \tag{8.41}$$

and

$$\zeta_i = \frac{\mathrm{Re}\lambda_i}{\omega_i} \tag{8.42}$$

Note that the key difference between the time domain approach to modal analysis and the frequency domain approach is that the time domain approach constructs a matrix from the time response and numerically computes the modal data by solving an eigenvalue problem. On the other hand, the frequency domain method extracts and curve-fits the modal data from the digital Fourier transform of the measured input and response data.

Two other major approaches in the time domain have been developed. One, called the polyreference method (Vold and Rocklin, 1982), again uses a state-space approach and has been developed commercially. The other time domain method is based on realization theory developed by control theorists, as introduced in Section 7.6. This method, advocated by Juang and Pappa (1985), also uses a state-space approach and is called the *eigensystem realization algorithm* (often abbreviated ERA). The eigensystem realization algorithm method introduces several important aspects to modal test analysis and hence is discussed next. The method is based on the realization theory introduced in Section 7.6 and puts modal testing on the firm theoretical foundation of linear systems theory (Juang, 1994).

Unlike the other time domain approaches, the eigensystem realization algorithm determines a complete state-space model of the structure under test. In particular, using the notation of Equations (7.1) and (7.2), the eigensystem realization algorithm identifies all three of the matrices A, B, and C. This is an important aspect because it addresses the nonuniqueness of modal analysis by specifying the measurement locations through the matrices B and C. In addition, the eigensystem realization algorithm approach firmly attaches the modal testing problem to the more mature discipline of realization used in control theory (Section 7.6). This approach is computationally more efficient and provides a systematic means of determining the order of the test model. The method is based on a discrete-time version of the state-space solution given by Equation (5.16) with $\mathbf{f}(\tau) = B\mathbf{u}(\tau)$. The solution of Equation (7.1), starting at time t_0, can be written as

$$\mathbf{x}(t) = e^{A(t-t_0)}\mathbf{x}(t_0) + \int_{t_0}^{t} e^{A(t-\tau)}B\mathbf{u}(\boldsymbol{\tau})\,d\boldsymbol{\tau} \tag{8.43}$$

This expression can be written at discrete time intervals equally spaced at times 0, $\Delta t, 2\Delta t, \ldots, k\Delta t, \ldots$, by making the substitutions $t = (k+1)\Delta t$ and $t_0 = k\Delta t$. This yields

$$\mathbf{x}((k+1)\Delta t) = e^{A\Delta t}\mathbf{x}(k\Delta t) + \int_{k\Delta t}^{(k+1)\Delta t} e^{A((k+1)\Delta t-\tau)}B\mathbf{u}(\tau)\,d\tau \tag{8.44}$$

Note that the integration period is now performed over a small increment of time, Δt. If $\mathbf{u}(t)$ is assumed to be constant over the interval Δt and to have the value $\mathbf{u}\ (k\Delta t)$, this last expression can be simplified to

$$\mathbf{x}(k+1) = e^{A\Delta t}\mathbf{x}(k) + \left[\int_0^{\Delta t} e^{A\sigma}\, d\sigma B\right]\mathbf{u}(k) \tag{8.45}$$

Here, $\mathbf{x}(k+1)$ is used to denote $\mathbf{x}((k+1)\Delta t)$, and so on, and the integration variable has been changed to $\sigma = (k+1)\Delta t - \tau$.

Equation (8.45) can be further reduced in form by defining two new matrices A' and B' by

$$A' = e^{A\,\Delta t}, \qquad B' = \int_0^{\Delta t} e^{A\sigma}\, d\sigma B \tag{8.46}$$

Thus, a discrete-time version of Equations (7.1) and (7.2) becomes

$$\begin{aligned} \mathbf{x}(k+1) &= A'\mathbf{x}(k) + B'\mathbf{u} \\ \mathbf{y}(k) &= C\mathbf{x}(k) \end{aligned} \tag{8.47}$$

The last expression allows the measurement taken at discrete times, $\mathbf{y}(k)$, to be related to the state matrix by the definition of the matrices A' and B'.

Consider a system subject to an impulse, $\mathbf{y}(1) = CB'\mathbf{u}(1)$, where $\mathbf{u}(1)$ is a vector of zeros and ones, depending upon where the impulse is applied. If the impulse is applied at m different points one at a time, all the response vectors at $k = 1, \mathbf{y}(k)$, corresponding to each of these m impulses, can be gathered together into a single $s \times m$ matrix Y, given by

$$Y(1) = CB' \tag{8.48}$$

In a similar fashioin, it can be shown using Equation (8.47) that for any measurement time k

$$Y(k) = CA^{k-1}B' \tag{8.49}$$

The matrices $Y(k)$ defined in this manner are called *Markov parameters*.

The Markov parameters for the test structure can next be used to define a larger matrix of measurements, denoted by $H_{ij}(k)$, for any arbitrary positive integers i and j by

$$H_{ij}(k) = \begin{bmatrix} Y(k) & Y(k+1) & \cdots & Y(k+j) \\ Y(k+1) & Y(k+2) & & \\ \vdots & \vdots & & \vdots \\ Y(k+i) & Y(k+u+1) & & Y(k+i+j) \end{bmatrix} \tag{8.50}$$

This $(i+1) \times (j+1)$ block matrix is called a *generalized Hankel matrix*. If the arbitrarily chosen integers $i+1$ and $j+1$ are both greater than $2n$, the rank of $H_{ij}(k)$ will be $2n$. This follows from realizing that the Hankel matrix can be factored and written as

$$H_{ij}(k) = O_i A^{k-1} R_j \tag{8.51}$$

where O_i is the observability matrix and R_j is the controllability matrix given by

$$O_i = \begin{bmatrix} C \\ CA' \\ \vdots \\ C(A')^i \end{bmatrix}, \qquad R_j = [B'A'B' \cdots (A')^j B'] \tag{8.52}$$

introduced in Section 7.2. Note that the rank of $H_{ij}(k)$ is the order of the matrix A', and hence the order of the system state matrix A, as long as i and j are large enough. Equation (8.52) also indicates that the smallest-order realization of A will have an order equal to the rank of O_i and R_j for a controllable and observable system. (Recall the balanced model reduction problem of Section 7.7.)

The eigensystem realization algorithm is based on a singular-value decomposition (see Section 7.7) of the Hankel matrix $H(0)$. Using Equation (7.60), the matrix $H(0)$ can be written as

$$H(0) = U\boldsymbol{\Sigma}V^T \tag{8.53}$$

where Σ is the diagonal matrix of the singular values, σ_i, of $H(0)$, and U and V are defined in Equations (7.60), (7.62), and (7.63). If enough measurements are taken, so that i and j are large enough, there will be an index r such that $\sigma_r >> \sigma_r + 1$. Just as in the model reduction problem of Section 7.7, this value of r yields a logical index for defining the order of the structure under test, i.e., $r = 2n$.

Partitioning U and V^T into the first r columns and rows respectively, and denoting the reduced matrices by U_r and V_r yields

$$H(0) = U_r \boldsymbol{\Sigma}_r V_r^T \tag{8.54}$$

Here, $\boldsymbol{\Sigma}_r$ denotes the $r \times r$ diagonal matrix of the first r singular values of $H(0)$. Juang and Pappa (1985) showed that

$$A' = \boldsymbol{\Sigma}_r^{-\min 1/2} U_r^T H(1) V_r \boldsymbol{\Sigma}_r^{-\min 1/2} \tag{8.55}$$

$$B' = \boldsymbol{\Sigma}_r^{1/2} V_r E_p \tag{8.56}$$

$$C = E_p^T U_r \boldsymbol{\Sigma}_r^{1/2} \tag{8.57}$$

where E_p is defined as the $p \times r$ matrix

$$E_p^T = [I_p \quad \mathbf{0}_p \quad \cdots \quad \mathbf{0}_p] \tag{8.58}$$

Here I_p is a $p \times p$ identity matrix and $\mathbf{0}_p$ is a $p \times p$ matrix of zeros.

The modal parameters of the test structure are calculated from the numerical eigensolution of the matrix A'. The mode shapes of the structure are taken from the eigenvectors of A', and the natural frequencies and damping ratios are taken from the eigenvalues of A.

The eigenvalues of A, the continuous-time state matrix, denoted by λ_i, are found from the eigenvalues of A' via the formula (see Juang and Pappa, 1985)

$$\lambda_i = \frac{\ln \lambda_i(A')}{\Delta t} \tag{8.59}$$

For underdamped structures, the modal parameters are determined from Equations (8.41) and (8.42).

8.7 MODEL IDENTIFICATION

A major reason for performing a modal test is for validation and verification of analytical models of the test structure. What is often desired is a mathematical model of the structure under consideration for the purpose of predicting how the structure will behave under a variety of different loadings, to provide the plant in a control design, or to aid in the design process in general. This section discusses three types of model of the structure that result from using modal test data. The three types of model considered are the *modal model*, discussed in the previous section, the *response model*, and the *physical model* (also called the *spatial model*).

The modal model is simply the natural frequencies, damping ratios, and mode shapes as given in the previous two sections. The modal model is useful in several ways. First, it can be used to generate both static and dynamic displays of the mode shapes, lending visual insight into the manner in which the structure vibrates. These displays are much more useful to examine, in many cases, than reading a list of numbers. An example of such a display is given in Figure 8.11.

A second use of modal models is for direct comparison with the predicted frequencies and modal data for an analytical model. Frequently, the analytical model will not predict the measured frequencies. As a result, the analytical model is changed, iteratively, until it produces the measured natural frequencies. The modified analytical model is then considered an improvement over the previous model. This procedure is referred to as model updating and is introduced in the following section.

The frequency response model of the system is given by the receptance matrix defined in Section 5.7 and used in Section 8.5 to extract the modal parameters from the measured frequency response functions. From Equations (5.68) and (5.65) the measured receptance

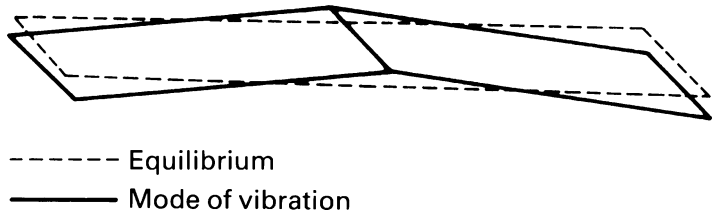

Figure 8.11 Display of the mode shape of a simple test structure.

matrix can be used to calculate the response of the test structure data to any input $\mathbf{f}(t)$. To see this, consider taking the Laplace transform, denoted £[·], of the dynamic equation (2.13), i.e.,

$$(s^2M + sD + K)\pounds[\mathbf{q}] = \pounds[\mathbf{f}] \tag{8.60}$$

so that

$$\pounds[\mathbf{q}(t)] = \frac{1}{s^2M + sD + K}\pounds[\mathbf{f}] \tag{8.61}$$

Letting $s = j\omega$ in Equation (8.61) yields

$$\Im(\mathbf{q}) = \alpha(\omega)\Im(\mathbf{f}) \tag{8.62}$$

where it is noted that the Laplace transform of a function evaluated at $s = j\omega$ yields the exponential Fourier transform, denoted by $\Im[.]$. Hence, Equation (8.62) predicts the response of the structure for any input $\mathbf{f}(t)$.

In some instances, such as control or design applications, it would be productive to have a physical model of the structure in spatial coordinates, i.e., a model of the form

$$M\ddot{\mathbf{q}} + D\dot{\mathbf{q}} + K\mathbf{q} = \mathbf{0} \tag{8.63}$$

where $\mathbf{q}(t)$ denotes a vector of physical positions on the structure. The obvious way to construct this type of model from measured data is to use the orthogonal mass normalized matrix of eigenvectors, S_m, defined in Section 3.5, and to 'undo' the theoretical modal analysis by using Equations (3.69) and (3.70). That is, if these equations are pre- and postmultiplied by the inverses of S_m^T and S_m, they yield

$$\begin{aligned} M &= (S_m^T)^{-1}S_m^{-1} \\ D &= (S_m^T)^{-1}\mathrm{diag}[2\zeta_i\omega_i]S_m^{-1} \\ K &= (S_m^T)^{-1}\mathrm{diag}[\omega_i^2]S_m^{-1} \end{aligned} \tag{8.64}$$

where the ω_i, ζ_i, and the columns of S_m are the measured modal data. Unfortunately, this formulation requires the damping mechanism to be proportional to velocity and measured data for all n modes to be available. These two assumptions are very seldom met. Usually, the modal data are too incomplete to form all S_m. In addition, the measured eigenvectors are seldom scaled properly.

The problem of calculating the mass, damping, and stiffness matrices from experimental data is very difficult and does not result in a unique solution (it is, after all, an inverse problem – see Lancaster and Maroulas, 1987, and Starek and Inman, 1997). Research continues in this area by examining reduced-order models and approaching the problem as one of improving existing analytical models, the topic of the next section.

8.8 MODEL UPDATING

Analytical models are only useful if they are verified against an experimental model. Often, analysis gets fairly close to predicting experimental data, and an approach called *model updating* is used to change slightly or update the analytical model to predict or agree with experimental data. Friswell and Mottershead (1995) present both an introduction to model updating and a good summary of most techniques developed up to that date. One approach to model updating is to use the analytical model of a structure to compute natural frequencies, damping ratios, and mode shapes, and then to test, or perform an experimental modal analysis on the structure and examine how well the analytical modal data predict the measured modal data. If there is some difference, then the analytical model is adjusted or updated until the updated analytical model predicts the measured frequencies and mode shapes. The procedure is illustrated by the following simple example.

Example 8.8.1

Suppose the analytical model of a structure is derived as the following two-degree-of-freedom model (from example 3.3.2):

$$I\ddot{\mathbf{q}}(t)+\begin{bmatrix} 3 & -1 \\ -1 & 1 \end{bmatrix}\mathbf{q}(t)=0$$

This has natural frequencies computed to be $\omega_1=\sqrt{2-\sqrt{2}}$ and $\omega_2=\sqrt{2+\sqrt{2}}$. Suppose a modal test is performed and that the measured frequencies are $\omega_1=\sqrt{2}$ and $\omega_2=\sqrt{3}$. Find adjustments to the analytical model such that the new updated model predicts the measured frequencies.

Let ΔK denote the desired correction in the analytical model. To this end, consider the correction matrix

$$\Delta K=\begin{bmatrix} 0 & 0 \\ \Delta k_1 & \Delta k_2 \end{bmatrix} \tag{8.65}$$

The characteristic equation of the updated model is then

$$\lambda^2-(4+\Delta k_1)\lambda+(2+3\Delta k_2+\Delta k_1)=0 \tag{8.66}$$

The characteristic equation of the system with the experimental frequencies would be

$$\lambda^2-5\lambda+6=0 \tag{8.67}$$

Comparing coefficients in Equations (8.66) and (8.67) yields the updated parameters

$$\Delta k_1=1 \qquad \text{and} \qquad \Delta k_2=1$$

The new updated model is

$$I\ddot{\mathbf{q}}(t)+\begin{bmatrix} 3 & -1 \\ 0 & 2 \end{bmatrix}\mathbf{q}(t)=0$$

which has frequencies $\omega_1=\sqrt{2}$ and $\omega_2=\sqrt{3}$ as measured.

While the updated model in example 8.8.1 does in fact produce the correct frequencies, the stiffness matrix of the updated model is no longer symmetric, nor does it retain the original connectivity of, in this case, the two-degree-of-freedom spring–mass system. Other methods exist that address these issues (see, for instance, Halevi, Tarazaga, and Inman, 2004). Model updating, as stated here, is related to the pole placement and eigenstructure assignment methods used in Section 7.3. Instead of computing control gains, as done in Section 7.3, the same computation yields an updating procedure if the gain matrices are considered to be the correction matrices (e.g., ΔK). Basically, if measured mode shapes, damping ratios, and frequencies are available, then an eigenstructure assignment method may be used to compute updated damping and stiffness matrices. If only damping ratios and frequencies are available, then pole placement can be used to update the damping and stiffness matrices. Friswell and Mottershead (1995) should be consulted for other methods. The literature should be consulted for latest approaches.

CHAPTER NOTES

Modal testing dominates the field of vibration testing. There are, of course, other identification methods and other types of vibration experiment. The main reference for this chapter is the text by Ewins (1984, 2000), which discusses each topic of this chapter, with the exception of Section 8.6 on time domain methods, in much more detail. Ewins (1984) was the first book to describe modal testing. Another good general reference for modal testing is the book by Zaveri (1984). Allemang (1984) has provided a review article on the topic as well as an extended bibliography. Each year since 1981, an International Modal Analysis Conference (IMAC) has been held, indicating the continued activity in this area. McConnell (1995) presents a more general look at vibration testing. Maia and Silva (1997) present an edited volume on modal analysis and testing written by Ewins' former students.

The material in Section 8.3 is a brief introduction to signal processing. More complete treatments along with the required material from Section 8.4 on random signals can be found in Otnes and Enochson (1972) or Doeblin (1980, 1983). An excellent introduction to signal processing and the appropriate transforms is the book by Newland (1985). There are many methods of extracting modal data from frequency response data, and only one is covered in Section 8.5. Ewins (2000) and Zaveri (1984) discuss others. Most commercially available modal software packages include details of the various modal data extraction methods used in the package.

The time domain methods are mentioned briefly in Ewins (2000) and by Allemang (1984). Leuridan, Brown, and Allemang (1986) discuss multiple-input and multiple-output time domain methods and present some comparison of methodology. However, the eigensystem realization algorithm is not included in these works. An excellent treatment of identification methods driven by structural dynamics is given in the text by Juang (1994). A good introduction to the realization theory upon which the eigensystem realization algorithm depends can be found in Chen (1970). A least-squares regression technique for system identification of discrete-time dynamic systems is given by Graupe (1976). The topic of physical modeling using measurements discussed in Section 8.7 is really an inverse problem and/or an identification problem such as defined in Rajaram and Junkins (1985) and Lancaster and Maroulas (1987). Virgin (2000) provides an excellent introduction to experimental

analysis for nonlinear systems. The use of vibration testing in structural health monitoring is reviewed in Doebling, Farrar, and Prime (1998). Inman *et al.* (2005) provide reviews of health monitoring and machinery diagnostics.

REFERENCES

Allemang, R.J. (1984) Experimental modal analysis. *Modal Testing and Refinement*, ASME-59, American Society of Mechanical Engineers, 1–129.

Blevins, R.D. (1994) *Flow Induced Vibration*, 2nd ed, Krieger Publishing, Malabar, Florida.

Chen, C.J. (1970) *Introduction to Linear System Theory*, Holt, Rinehart & Winston, New York.

Cole, D.G., Saunders, W.R., and Robertshaw, H.H. (1995) Modal parameter estimation for piezostructures. *Trans. ASME, Journal of Vibration and Acoustics*, **117** (4), 431–8.

Cooley, J.W. and Tukey, J.W. (1965) An algorithm for the machine calculation of complex fourier series. *Mathematics of Computation*. **19** (90), 297–311.

Doeblin, E.O. (1980) *System Modeling and Response: Theoretical and Experimental Approaches,* John Wiley & Sons, Inc., New York.

Doeblin, E.O. (1983) *Measurement Systems Application and Design*, 3rd ed, McGraw-Hill, New York.

Doebling, S.S., Farrar, C.R., and Prime, M.B. (1998) A summary review of vibration-based damage identification methods. *The Shock and Vibration Digest,* **30**, 91–105.

Ewins, D.J. (1984) *Modal Testing: Theory and Practice*, Research Studies Press, Baldock, Hertfordshire, UK.

Ewins, D.J. (2000) *Modal Testing: Theory and Practice*, 2nd ed, Research Studies Press, Baldock, Hertfordshire, UK.

Friswell, M.I. and Mottershead, J.E. (1995) *Finite Element Updating in Structural Dynamics*, Kluwer Academic Publications, Dordrecht, the Netherlands.

Graupe, D. (1976) *Identification of Systems*, R. E. Krieger Publishing Co., Melbourne, Florida.

Halevi, Y., Tarazaga, P.A., and Inman, D.J. (2004) Connectivity constrained reference basis model updating. Proceedings of ISMA 2004 International Conference on *Noise and Vibration*, Leuven, Belgium, 19–22, September 2004, on CD.

Ibrahim, S.R. (1973) A time domain vibration test technique, PhD Diss., Department of Mechanical Engineering, University of Calgary, Alberta, Canada.

Ibrahim, S.R. and Mikulcik, E.C. (1976) The experimental determination of vibration parameters from time responses. *Shock and Vibration Bulletin*, (46), Part 5, 187–96.

Inman, D.J., Farrar, C.R., Steffen Jr, V., and Lopes, V. (eds) (2005) *Damage Prognosis*, John Wiley & Sons, Inc., New York.

Juang, J.-N. (1994) *Applied System Identification*, Prentice-Hall, Upper Saddle River, New Jersey.

Juang, J.-N. and Pappa, R. (1985) An eigensystem realization algorithm for modal parameter identification and modal reduction. *AIAA Journal of Guidance, Control, and Dynamics*, **8**, 620–7.

Lancaster, P. and Maroulas, J. (1987) Inverse eigenvalue problems for damped vibrating Systems. *Journal of Mathematical Analysis and Application*, **123** (1), 238–61.

Leuridan, J.M., Brown, D.L., and Allemang, R.J. (1986) Time domain parameter identification methods for linear modal analysis: a unifying approach. *Trans. ASME, Journal of Vibration, Acoustics, Stress, and Reliability in Design*, **108**, 1–8.

Maia, N.M.M. and Silva, J.M.M. (1997) *Theoretical and Experimental Modal Analysis*, Research Studies Press, Baldock, Hertfordshire, UK.

McConnell, K.G. (1995) *Vibration Testing; Theory and Practice*, John Wiley & Sons, Inc., New York.

Newland, D.E. (1985) *An Introduction to Random Vibrations and Spectral Analysis*. 2nd ed, Longman Group Ltd, London.

Otnes, R.K. and Enochson, L. (1972) *Digital Time Series Analysis*, John Wiley & Sons, Inc., New York.

Rajaram, S. and Junkins, J.L. (1985) Identification of vibrating flexible structures. *AIAA Journal of Guidance Control and Dynamics*, **8** (4), 463–70.

Starek, L. and Inman, D.J. (1997) A symmetric inverse vibration problem for nonproportional, underdamped systems. *Trans. ASME, Journal of Applied Mechanics*, **64** (3), 601–5.

Virgin, L.N. (2000) *Introduction to Experimental Nonlinear Dynamics*, Cambridge University Press, Cambridge, UK.

Vold, H. and Rocklin, T. (1982) The numerical implementation of a multi-input modal estimation algorithm for mini computers. Proceedings of 1st International Modal Analysis Conference, 542–8.

Zaveri, K. (1984) *Modal Analysis of Large Structures – Multiple Exciter Systems*. Bruel and Kjaar Publications, Naerum.

PROBLEMS

8.1 Plot the error in measuring the natural frequency of a single-degree-of-freedom system of mass 10 and stiffness 35 if the mass of the exciter is included in the calculation and ranges from 0.4 to 5.0.

8.2 Calculate the Fourier transform of $f(t) = 3\sin 2t + 2\sin t - \cos t$ and plot the spectral coefficients.

8.3 Consider a signal $x(t)$ with a maximum frequency of 500 Hz. Discuss the choice of record length and sampling interval.

8.4 The eigenvalues and mode shapes of a structure are given next. Develop a two-degree-of-freedom model of the structure that yields the same modal data if the mass matrix is known to be diag[4 1]:

$$\lambda_1 = -0.2134 \pm 1.2890j$$
$$\lambda_2 = -0.0366 \pm 0.5400j$$
$$\mathbf{u}_1 = [0.4142 \quad 1]^T$$
$$\mathbf{u}_2 = [1.000 \quad -0.4142]^T$$

8.5 Consider the vector $\mathbf{s}^T = [s_1 \ s_2 \ s_3]$. Write the outer product matrix $\mathbf{s}\mathbf{s}^T$ and show that the elements in one row (or one column) of the matrix completely determine the other six elements of the matrix. In particular, calculate the receptance matrix of Section 8.5 for the following measured data:

$\zeta_1 = 0.01,$	$\zeta_2 = 0.2,$	$\zeta_3 = 0.01$	
$\omega_{d1} = 2,$	$\omega_{d2} = 10,$	$\omega_{d3} = 12$	
$G(\omega_{d1}) = 1,$	$G(\omega_{d2}) = -1,$	$G(\omega_3) = 3$	(force at position 1 and transducer at position 3)
$G(\omega_{d1}) = -3,$	$G(\omega_{d2}) = 2,$	$G(\omega_{d3}) = 4$	(force at 1, transducer at 2)
$G(\omega_{d1}) = 5,$	$G(\omega_{d2}) = 2,$	$G(\omega_{d3}) = -2$	(force at 1, transducer at 1)

What are the eigenvectors of the system?

8.6 Calculate the receptance matrix for the two-degree-of-freedom system with

$$M = \begin{bmatrix} 5 & 0 \\ 0 & 10 \end{bmatrix}, \qquad K = \begin{bmatrix} 4 & -2 \\ -2 & 6 \end{bmatrix}, \qquad D = \begin{bmatrix} 6 & -4 \\ -4 & 5 \end{bmatrix}$$

8.7 (**a**) Consider the system of problem 8.6. Using any integration package, numerically solve for the free response of this system to the initial conditions $\mathbf{q}(0) = [1\ 0]^T$ and $\dot{\mathbf{q}}(0) = [0\ 0]^T$.

(**b**) Using the solution to (a), generate the matrices Φ and Φ' of Equations (8.33) and (8.34). Using Φ and Φ' and Equation (8.38), calculate the eigenvalues and eigenvectors of the system. Check to see if they satisfy the eigenvalue problem for this system.

8.8 Repeat problem 8.7 using ERA. This will require the availability of software performing SVD, and the like, such as MATLAB.

8.9 Solve the problem of example 8.1.1 again for the case where the measured frequencies are $\omega_1 = \sqrt{2}$ and $\omega_2 = 2$.

8.10 Solve the model updating problem of example 8.8.1 using the pole placement method of Sections 6.6 and 7.3 to see if it is possible to obtain a symmetric updated stiffness matrix with the required eigenvalues.